Grant Agreement Number: 952183
Project Acronym: BOW
Project Full Title: Biogenic Organotropic Wetsuits
Start date of the project: November 1st, 2020
Duration: 48 months
Project Coordinator: Paolo Bergese (CSGI)
Project Officer: Ioannis Amarantos
Project Website: www.bowproject.eu
Project e-mail address: bow@csgi.unifi.it

D4.4: evBOW products in *C. elegans*

DELIVERABLE INFORMATION	
Deliverable N°	4.4
Deliverable Title	evBOW products in *C. elegans*
WP N°	4
Lead beneficiary	CNR
Contributing partners	CSGI, HMGU, USC, UMORE
Type	Report
Lead authors	Elia Di Schiavi (CNR)
Due Submission Date	30/04/2024
Actual Submission Date	30/04/2024

TYPE		
R	Document, report	☒
DEM	Demonstrator, pilot, prototype	☐
DEC	Websites, patent filing, videos, etc.	☐
OTHER		☐

This project has received funding from the European Union's Horizon 2020 research and innovation programme under grant agreement No 952183

DISSEMINATION LEVEL		
PU	Public	☒
PP	Restricted to other programme participants (incl. Commission Services)	☐
RE	Restricted to a group specified by the consortium (incl. Commission Services)	☐
CO	Confidential, only for the members of the consortium (incl. Commission Services)	☐

STATUS	
Draft	☐
Final	☒

REVISION HISTORY		
Date	**Authors and Contributors**	**Comments**
11/04/2024	Pamela Santonicola (CNR), Elia Di Schiavi (CNR)	First Draft
15/04/2024	Sebastiano Di Bucchianico (HMGU)	Review and editing of the first draft
22/04/2024	Miriam Romano (CSGI) and Paolo Bergese (CSGI)	Review and editing of the first draft
29/04/2024	Pamela Santonicola (CNR), Elia Di Schiavi (CNR)	Second draft
30/04/2024	Miriam Romano (CSGI), Paolo Bergese (CSGI), Irene Trapani (CSGI)	Review and editing, final version

GLOSSARY OF TERMS	
TERM	**DEFINITION**
BOW	Biogenic Organotropic Wetsuits
WP	Work package
EVs	Extracellular Vesicles
MBD	Magnetic Bead Device
NPs	Nanoparticles
MBDs-PDA	Magnetic Bead Devices functionalized with polydopamine
s.c. MBDs	Single core Magnetic Bead Devices
m.c. MBDs	Multi core Magnetic Bead Devices
MGAP-19	Selected prototype of s.c. MBDs
AP-20	Selected prototype of m.c. MBDs
evMBDs	EV membrane coated MBDs
EDT-MSCs	Human endometrial decidual tissue derived mesenchymal stromal/stem cells
MSC-EVs	EVs produced by EDT-MSCs

This project has received funding from the European Union's Horizon 2020 research and innovation programme under grant agreement No 952183

RBCs	Red Blood Cells
RBC-EVs	Red Blood Cells-derived EVs
lpMBDs	Liposome-membrane coated MBDs
Alg	Nanoalgosomes
ICP-AES	Inductively Coupled Plasma atomic emission spectroscopy
NAC	N-AcetylCysteine
H_2O_2	Hydrogen Peroxide
PBS	Phosphate-buffered saline
H_2O	Water
SEM	Standard Error of the Mean
GFP	Green Fluorescent Protein
DsRed	Red Fluorescent Protein
PDA	Polydopamine
RITC	Rhodamine B isothiocyanate
LGM	Liquid Growth Medium

This project has received funding from the European Union's Horizon 2020 research and innovation programme under grant agreement No 952183

The statements made herein do not necessarily have the consent or agreement of the BOW consortium.

This project has received funding from the European Union's Horizon 2020 research and innovation programme under grant agreement No 952183

INDEX

This project has received funding from the European Union's Horizon 2020 research and innovation programme under grant agreement No 952183

1. INTRODUCTION

1.1 OVERVIEW AND APPLICATIONS

This deliverable refers to WP4, whose primary objective is to assess the biological efficacy and toxicity of the EV-membrane coated magnetic bead devices (evMBDs) by evaluating their *in vitro*, *ex vivo*, and *in vivo* performance. In particular, it reports on Task 4.4 activities (M13-M42) focused on testing *in vivo* in the model system *Caenorhabditis elegans* the biocompatibility and biodistribution of BOW products. These include EVs from *Tetraselmis chuii* microalgae (nanoalgosomes), and EVs from human endometrial decidual tissue derived mesenchymal stromal/stem cells (MSCs-EVs), Red Blood Cells-derived Extracellular Vesicles (RBC-EVs) as well as single core MBDs (s.c. MBDs) and multi core MBDs (m.c. MBDs). T4.4 have also performed experiments on liposome-coated MBDs (lpMBDs) as a proxy model of evMBDs (see 2nd Periodic Technical Report, Part B). Since it is not clear whether EV cargo will be completely removed during the encapsulation process of MBDs, it is of foremost importance to study EV bioactivity *per se* in whole animal models. For these reasons, *C. elegans* was used to facilitate rapid, high-throughput uptake, distribution, and toxicological tests *in vivo,* as a first screening step in a whole living organism, prior to the use of mammalian models. This approach also allows to fulfil the 4R principles for higher animal use (Replacement, Reduction, Refinement, Rehabilitation), a theme highly supported by EU.

2. MATERIAL AND METHODS

2.1 *C. ELEGANS* MAINTENANCE AND STRAINS

Nematodes have been grown and handled following standard procedures under uncrowded conditions on nematode growth medium (NGM) agar plates seeded with *Escherichia coli* strain OP50 (Brenner, 1974), unless otherwise specified (Picciotto *et al.*, 2022; Romano *et al.*, 2023). List of the strains used: wild-type strain N2 (Bristol variety); EG1285 *oxIs12* X *[unc-47p::GFP; lin-15(+)]* (expression of the Green Fluorescent Protein, GFP, in GABA neurons); QH3803 *vdEx263 [mec-4p::mCherry; odr-1p::dsRed]* (expressing mCherry in mechanosensory neurons); BY250 *vtIs7 [dat-1p::GFP]* (expressing GFP in dopaminergic neurons); VC2405 *chc-1(ok2369) III/hT2 [bli-4(e937) let-?(q782) qIs48]* (I;III) (knockout mutant of *chc-1*); RT1315 *unc-119(ed3) III,* RT476 *unc-119(ed3) III; pwIs170 [vha6p::GFP::rab-7 + Cbr-unc-119(+)] (*expression of an intestine-specific GFP marker for late endosomes); CL2166 *dvIs19 III [(pAF15) gst-4p::GFP::NLS]* (expression of an oxidative stress-responsive GFP).

2.2 *IN VIVO* BIODISTRIBUTION AND PERSISTENCE

Wild-type, transgenic or mutant animals were treated with labelled EVs, MBDs and lpMBDs *in solido* (feeding) or *in liquido* (soaking) (Picciotto *et al.*, 2022). For biodistribution assays ~20-30 synchronized L4 larvae were transferred on freshly prepared NGM plates seeded with heat-killed OP50 bacteria or in 96-well plates with LGM [OP50 bacteria, M9 buffer, antibiotic antimycotic solution 2x (cat. n. A5955 Sigma-Aldrich®) and cholesterol 5ng/ml] and NPs. After 24- or 48h of treatment in the dark, young adult animals were transferred to clean NGM plates with OP50 bacteria to let the animals crawl for 1 h to

This project has received funding from the European Union's Horizon 2020 research and innovation programme under grant agreement No 952183

remove the excess of dye. Animals were immobilized with 0.01% tetramisole hydrochloride (Sigma-Aldrich, T1512) on 4% agar pads for microscopy analysis and confocal images were collected with a Leica TCS SP8 AOBS microscope using a 40x objective. To assess NPs persistence, animals have been analyzed every 24h after the interruption of the treatment.

2.3 BIOCOMPATIBILITY *IN VIVO* ASSAYS

For the assessment of NPs toxicity *in vivo*, *C. elegans* synchronized animals have been treated with mock or NPs (concentrations indicated in the figure legend of each experiment), through *in liquido* culturing in 96-multiwell plates for 72 h (Picciotto *et al.,* 2022; Romano *et al*., 2023). Synchronized eggs were obtained by bleaching and resuspended in LGM. 60 µL of this mix containing approximately a total of 30 eggs were aliquoted in each well. After 72 h the number of living animals and of animals reaching the adult stage was quantified per each replicate, with a minimum number of replicates corresponding to three. For the lifespan assay, synchronized animals have been treated *in solido*, as described above. Viability was scored every 3 days and animals were transferred every 3 days in fresh plates. To test NPs effect on brood size and embryonic vitality, 20 animals were treated *in solido* in triplicate, as described above, until L4 larval stage and then transferred to new plates without any treatment. Then, every 24 h animals were moved to new plates without any treatment for all the fertile period of the animals (4 days) and the number of laid and hatched eggs counted every day. To test NPs effect on animal movement, a thrashing assay was performed on young adult hermaphrodite right after the treatment or 24 and 48h after treatment to assess NPs persistence. Animals were transferred in 7µL of M9 buffer, left 5 minutes in buffer and then video recorded for 30 seconds. The measurement of thrashing was done counting every change of direction respect to the longitudinal axis of the body. To assess a putative NPs neurotoxicity, animals expressing fluorescent protein in GABAergic, mechanosensory and dopaminergic neurons were treated *in liquido* in triplicate, as described above. After 72 h of treatment animals were immobilized as above and the morphology and the total number of visible fluorescent neurons was quantified in each animal. Confocal images were collected with a Leica TCS SP8 AOBS microscope using a 20x objective. To determine iron internalization animals have been treated *in liquido* as described above and after 0- and 48h post treatment 300-500 animals have been manually collected in 50µL of H_2O for iron quantification by ICP-AES.

2.4 ANTIOXIDANT BIOACTIVITY ASSAYS

For the assessment of exogenous H_2O_2 stress response, animals have been treated *in liquido* as described above for 72 h with NPs, and N-AcetylCysteine (NAC) (Sigma-Aldrich, A7250) 2mM as positive control (Bongiovanni *et al*., 2023). After treatment, animals were exposed to H_2O_2 5 mM and water as control for 2 h, then transferred to fresh NGM plates with OP50 bacteria and the number of moving animals on the total number of animals on the plate was scored.

This project has received funding from the European Union's Horizon 2020 research and innovation programme under grant agreement No 952183

gst-4p::GFP total expression was quantified after 72 h of treatment *in liquido* with NPs, as described above. 5 animals on each slide were immobilized using 100 mM NaN_3 (Sigma-Aldrich, S8032) to allow the lineup of animals. Epi-fluorescence images were collected with a Leica TCS SP8 AOBS inverted microscope, using a 10x objective and FITC filter. Fluorescence quantification was performed using ImageJ, and the Corrected Total Fluorescence (CTF) was calculated for each image using this formula: (integrated density of the area containing the animals) – [(area containing the animals) x (mean fluorescence of background)]. The anti-aging effect of NPs on animal movement was assessed through the thrashing assay on young (3 days from hatching) and old (10 days from hatching). Animals at young adult stage have been treated for 16 h *in liquido*, then transferred to fresh NGM plates and young animals ~~were~~ have been immediately analyzed, while old animals ~~were~~ have been transferred every 2 days in fresh plates until day 10 from hatching. For video recording animals were transferred in 7µL of M9 buffer, left 5 minutes to acclimate and then recorded for 30 seconds. The measurement of thrashing was done counting every change of direction respect to the longitudinal axis of the body. Treatments were performed in triplicate.

3. NANOALGOSOME PERFORMANCES *IN VIVO* IN *C. ELEGANS*

3.1 NANOALGOSOME BIOACTIVITY

The model system *C. elegans* was used to test *in vivo* nanoalgosome biocompatibility assessing the organismal responses (i.e., viability, growth, neuron survival and lifespan). Chronic treatments were performed exposing the animals from eggs until adult stage (72h) using different nanoalgosome concentrations (1, 20, 64 and 128 ng/µL) and two different methodologies for administration (soaking and feeding) that depend on the kind of assay (Picciotto *et al.*, 2022). Nanoalgosomes have been provided by BOW partners producing and delivering nanoalgosomes (Alg, WP1, D1.2 and D1.4). Nanoalgosome toxicity was assessed by looking at the effect on animal survival and growth, not observing any toxic effect at all the concentrations tested after 72 hours, when all untreated animals are alive and reached the adult stage (Figure 1a and b). Interestingly, nanoalgosomes increase animal motility in a dose-dependent manner and the minimum efficient concentration resulted to be 20 ng/µL in the thrashing assay, a test that measures animal swimming in water in 1 minute (Figure 1c). This experiment was also useful to determine the minimal effective concentration (20 ng/µL) efficient in increasing animal motility without causing any toxic effect, thus we decided to use this concentration for further experiments. Since it is known that in *C. elegans* antioxidant molecules are capable to influence animal motility (Sugawara *et al.,* 2020) and that microalgae are sources of antioxidant compounds (Plaza *et al.,* 2009), a possible antioxidant effect of nanoalgosomes was investigated *in vivo.* At first, animals have been exposed to an exogenous oxidative stress (H_2O_2 5mM), which induced a severe reduction of motility. Interestingly, a pre-treatment with nanoalgosomes counteracted this oxidative stress and reduced H_2O_2 toxic effects (Figure 1d), similarly to N-AcetylCysteine (NAC), an antioxidant agent used as positive control. A transgenic strain expressing the GFP under the control of the *gst-4* promoter, the ortholog of glutathione S-

This project has received funding from the European Union's Horizon 2020 research and innovation programme under grant agreement No 952183

transferase, was used to confirm the capability of nanoalgosomes to modulate the expression of a detoxifying gene that is activated in response to oxidative stress. *gst-4* indeed was found downregulated after treatment with nanoalgosomes (Figure 1e, see 5.2). Since antioxidant molecules counteract also aging impact on locomotion, the anti-aging properties of nanoalgosomes were investigated by looking at animal movement decline during aging. Interestingly, nanoalgosomes prevented the effects of aging by preserving the movement capability in older animals (3 days after adulthood) and keeping it at the same level to the one observed in younger animals (adults) (Figure 1f).

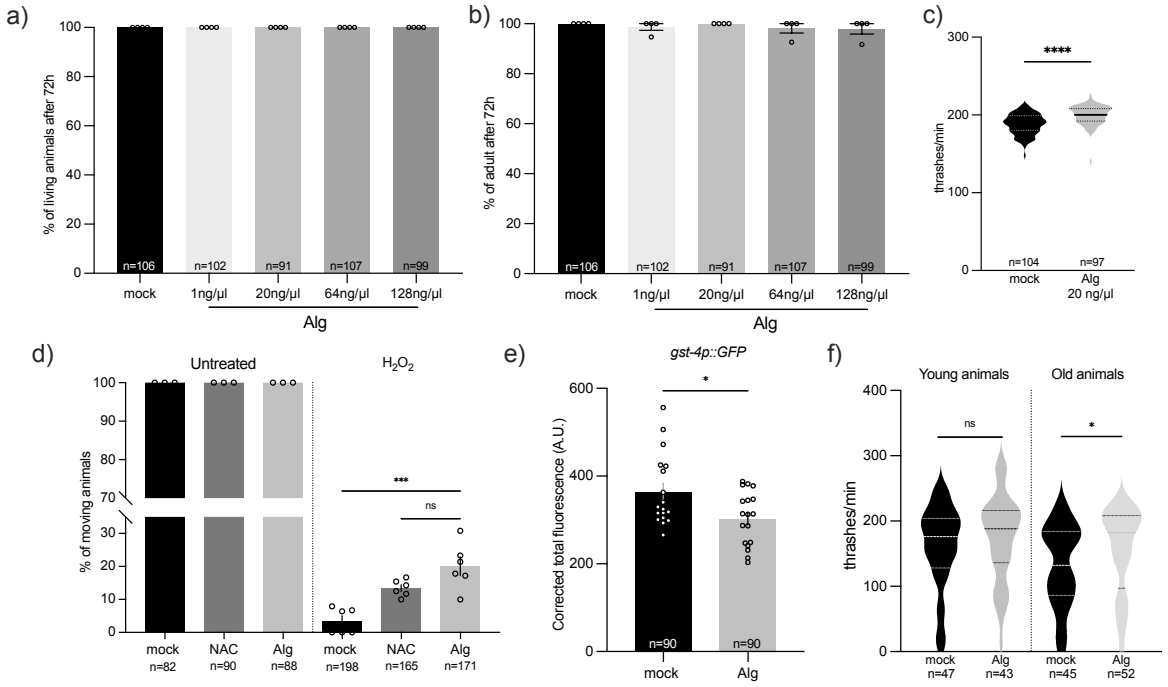

Figure 1. *a) Quantification of the number of living animals after treatment with mock (PBS) or nanoalgosomes (Alg) at different concentrations. b) Quantification of the number of animals reaching adult stage after treatment with mock or nanoalgosomes at different concentrations. c) Quantification of the number of thrashes (locomotion) after chronic treatment with mock and nanoalgosomes. d) In vivo response to exogenous oxidative stress. Animals have been pre-treated with mock, NAC (2 mM) or nanoalgosomes. Animal movement was assessed right after an acute exposure with H_2O (untreated) or H_2O_2 5 mM. e) Quantification of the fluorescence in gst-4p::GFP expressing animals after chronic treatment with mock or nanoalgosomes. f) Thrashing assay on young and old animals after acute treatments (16h) with mock and nanoalgosomes (10 ng/µL). Bars represent the means and dots the replicates (in a, b, d) or the total fluorescence in a picture corrected for the background (e), error bar is the SEM. Violin plots (c and f) show the distribution of thrashes performed by the animals in a minute; bold dashed lines in the centre correspond to the medians, while upper and lower dashed lines correspond to the quartiles. n is the number of animals analysed. Nanoalgosome concentration used was 20 ng/µL corresponding to $1e^9$ particles/mL, unless differently indicated. Only statistically significant differences have been reported using t-test (c, e and f), One-way ANOVA (a, b and d) *p≤0.05; ***p<0.005; ****p<0.0001; ns>0.05.*

This project has received funding from the European Union's Horizon 2020 research and innovation programme under grant agreement No 952183

To further assess nanoalgosome toxicity, animals were treated over their entire lifespan and no effect was observed on their survival curve (Figure 2a). Moreover, exposure to nanoalgosomes did not alter animal fertility (Figure 2b) or offspring survival (Figure 2c), confirming that the absence of any transgenerational effect. Moreover, to evaluate the putative neurotoxicity of nanoalgosomes, neuronal survival was assessed. *C. elegans'* transparency allows to observe specific cell types, such as neurons, in living adult animals by using fluorescent proteins that are only expressed in the cells of interest when they are viable. Moreover, the invariant cell lineage in *C. elegans* allows to have a fixed number of cells in *C. elegans* adults, which corresponds to a total of 959 somatic cells, including 302 neurons, in every wild-type animal. Nanoalgosome neurotoxicity was evaluated on three different neuronal classes, the 19 GABAergic motoneurons, the 6 dopaminergic sensory neurons, and the 6 glutamatergic mechanosensory neurons and no effect was observed on neuronal survival (Figure 2d, e, f).

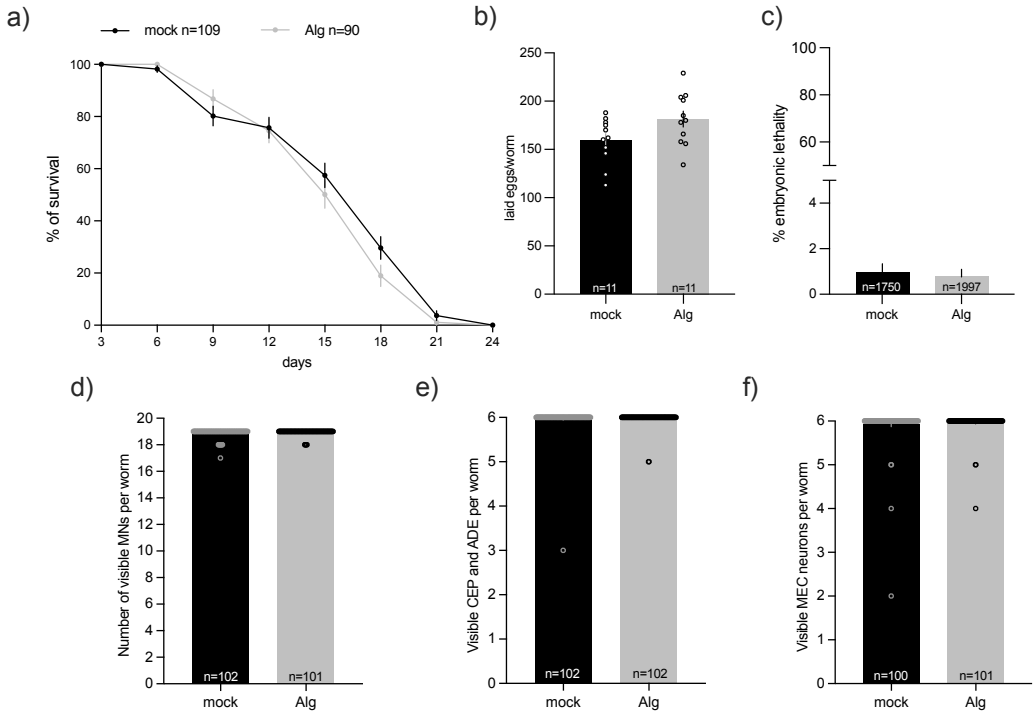

Figure 2. *a) Lifespan of animals treated with mock and nanoalgosomes (Alg). b) Brood size of single animals after treatment with mock and nanoalgosomes. c) Embryonic lethality of eggs after treatment of parental strain with mock and nanoalgosomes. g-i) Quantification of the number of 19 visible motoneurons (MNs), 6 dopaminergic neurons in the head (CEP and ADE) and 6 mechanosensory neurons (MEC) expressing GFP, after treatment with mock and nanoalgosomes. Kaplan-Meier curve (a); bars represent the means and dots the replicates (b-f). SEM is shown in all graphs. n is the number of animals analysed (a, d-f) or the number of P0 animals (b), or the number of eggs analysed (c). Nanoalgosome concentration used was 20 ng/µL corresponding to 1e^9 particles/mL. t-test (b-f) and Log-rank Mantel-Cox (a) was used and no statistically significant differences were found.*

Taken together these results suggest a high biocompatibility of nanoalgosomes in living animals, with no major toxic effect at the tested concentrations. Moreover, nanoalgosome

This project has received funding from the European Union's Horizon 2020 research and innovation programme under grant agreement No 952183

intrinsic antioxidant and anti-aging properties have been tested *in vivo*. Some of these results together with the ones obtained by BOW project partners are part of a manuscript available online as pre-print (Bongiovanni *et al.*, 2023) and under third revision in Communications Biology.

3.2 NANOALGOSOME BIODISTRIBUTION AND STABILITY

C. elegans body transparency allows to visualize, in a whole living animal, nanoparticle biodistribution. Taking advantage of transgenic animals expressing the GFP in specific tissues or cellular compartments (available at CNR IBBR), it was also possible to establish the targeted tissue. As reported in the paper Picciotto *et al.*, 2022, different methodologies (soaking, feeding and injection) have been explored for animal treatment and both feeding and soaking methods resulted to be the most suitable and fast for this purpose. After 24 h of treatment by feeding with nanoalgosomes labelled with two different lipophilic dyes (Di-8-anepps or PKH26) a fluorescent signal was observed in the intestinal cells of all the animals (arrow) and in some head and tail neurons (asterisks) (Figure 3a). No signal was observed with unlabeled nanoalgosomes or lipophilic dyes alone. To corroborate the specificity and purity of labelled-nanoalgosome, a sucrose density gradient was performed to exclude the presence of free dye or dye aggregates and a similar localization was observed in the worms. The fluorescent signal localizes in the cytoplasm of intestinal cells (Figure 3b) and co-localizes with late endosomal markers (Figure 3c). Interestingly, fluorescent nanoalgosomes showed a tropism for neurons (Figure 3a), that was not observed using other types of EVs (see section 3 and 4). To determine nanoalgosome internalization mechanisms in the intestinal cells, animals impaired for the clathrin-mediated endocytosis have been used. These animals carry a lethal mutation in the heavy chain of clathrin (*chc-1 KO)*. *chc-1 KO* heterozygote mutant animals exposed to fluorescent nanoalgosomes showed a strong reduction in the fluorescence signal compared to wild-type animals (Figure 3d), suggesting that fluorescent nanoalgosomes are internalized in *C. elegans* via clathrin-mediated endocytosis.

To assess nanoalgosome stability, a treatment was performed for 24 h with Di-8-anepps fluorescently labelled nanoalgosomes and, after interrupting the treatment, the fluorescent signal in the intestinal cells was observed every 24 h for 3 days. Interestingly, nanoalgosomes resulted to be highly stable *in vivo* in *C. elegans,* since the fluorescent signal was visible up to 72 h post treatment (Figure 4), a time corresponding to the entire fertile period of the animal.

This project has received funding from the European Union's Horizon 2020 research and innovation programme under grant agreement No 952183

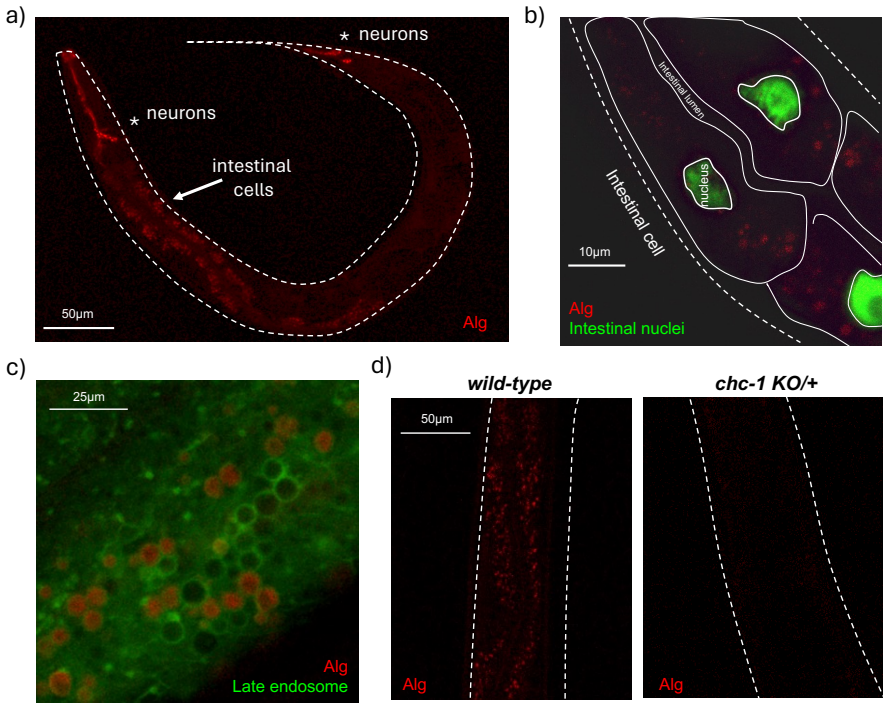

Figure 3. *a) Representative confocal images of wild-type animals treated with Di-8-anneps nanoalgosomes (Alg, red). b) Representative confocal images of transgenic animals expressing GFP in intestinal nuclei (elt-2p::NLS::GFP, green) treated with Di-8-anneps nanoalgosomes (red). c) Representative confocal images of transgenic animals expressing GFP in late endosomes of intestinal cells (vha-6p:: GFP::RAB-7, green) treated with Di-8-anneps nanoalgosomes (red). d) Representative confocal images of wild-type animals and* chc-1 KO/+ *heterozygote animals treated with Di-8-anneps nanoalgosomes (red). Nanoalgosome concentration used was 20 ng/µL corresponding to* $1e^9$ *particles/mL. Animal body is outlined with white dashed lines, with heads located on the left (a) or up (b, d). Scale bars are reported in the images.*

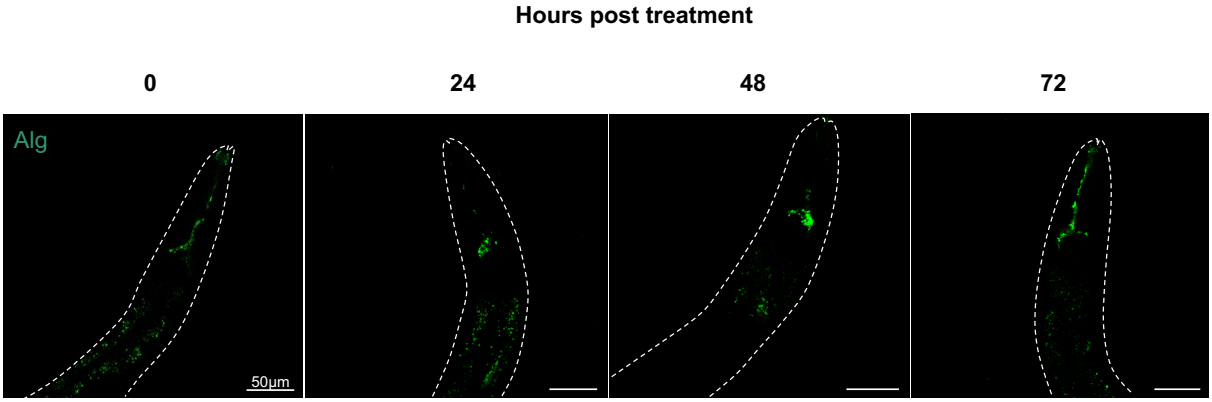

Figure 4. *Representative confocal images of the heads of wild-type animals treated with Di-8-anneps nanoalgosomes (green) and observed at 0-, 24-, 48- and 72-hours post-treatment. The nanoalgosome concentration used was 20 ng/µL corresponding to* $1e^9$ *particles/mL. Animal body is outlined with white dashed lines. Scale bars are reported in the images.*

This project has received funding from the European Union's Horizon 2020 research and innovation programme under grant agreement No 952183

All these results together with the ones obtained by BOW project partners are part of a published manuscript (Picciotto *et al.*, 2022) and of another available online as pre-print (Bongiovanni *et al.*, 2023) and under third revision in Communications Biology.
Taken together all these results strongly support the use of nanoalgosomes to encapsulate MBDs.

4. MSC-EV BIODISTRIBUTION *IN VIVO* IN *C. ELEGANS*

We assessed the biodistribution of mesenchymal stromal/stem cells EVs (MSC-EVs) (provided by *RIGENERAND* partner, WP1, D1.1 and D1.4) produced by cells expressing DsRed in the cytoplasm. Animals have been treated for 24h with 20 ng/µL of MSC-EVs DsRed, using the same protocol described in paragraph 2.2. After 24h no fluorescent signal was observed inside the animal, unlike what observed with nanoalgosomes. Therefore, animals have been treated for 48h with MSC-EVs DsRed and a red fluorescent signal in the intestinal cells of all the animals was observed (Figure 5), suggesting an interesting difference in the time needed by worms to uptake EVs from different sources. This result further confirms the consistency of the fluorescent signal observed in the intestine after treatment of *C. elegans* with EVs differently labelled. Despite the promising results, no further experiments have been performed so far with MSC-EVs since the shortage caused by the change of partner in the consortium in charge of their production.

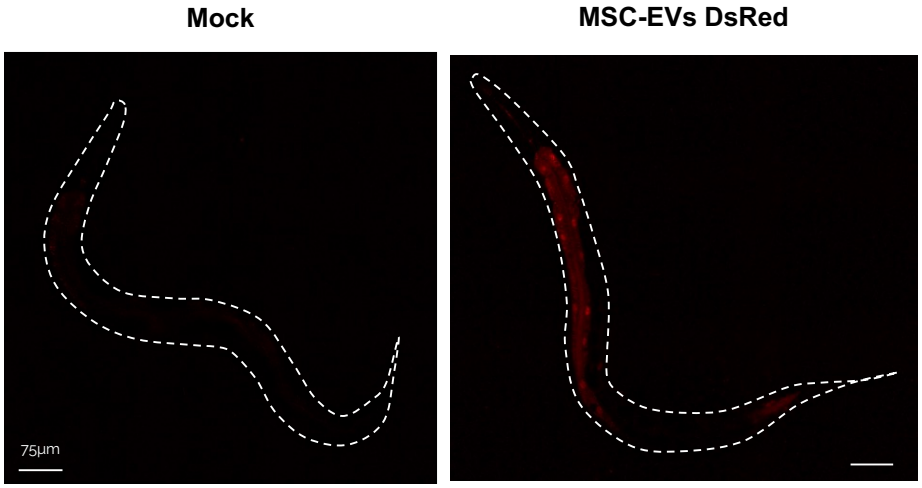

Figure 5. *Representative confocal images of animals treated with MSC-EVs DsRed (red) (20 ng/µL corresponding to 6e^6 particles/mL). Animal body is outlined with white dashed lines, head is up. Scale bars are reported in the images.*

5. RBC-EV PERFORMANCES *IN VIVO* IN *C. ELEGANS*

Red Blood Cells-derived EVs (RBC-EVs) (produced and provided by the CSGI partner by the protocols described in Musicò A, *et al.* 2023) were initially not included in the GA but have been introduced as a contingency plan to face the shortage in MSC-EVs. Moreover, the external scientific advisory board also strongly supported the use of RBC-EVs (see Annex 2).

This project has received funding from the European Union's Horizon 2020 research and innovation programme under grant agreement No 952183

5.1 RBC-EVs BIOACTIVITY

Based on the experiments performed with nanoalgosomes, RBC-EVs have been tested for their effect on animal movement. Chronic treatment (72h) of the animals with 20 ng/µL of RBC-EVs increases animal movement (Figure 6).

A dose-response effect of RBC-EVs on thrashing was also assessed and all the doses tested (1, 20, 60 and 128 ng/µL) increased animal movement, with a very high increase observed with the highest concentration (mean of 332 thrashes/min, *****p<0.0001 vs* 20 ng/µL*)*. RBC-EVs preparations resulted to be very consistent, since samples isolated from different donors increased animal movement in a similar way. The effect observed on animal movement can be associated with the abundant presence of antioxidant enzymes in the RBCs, an aspect that deserves further investigations.

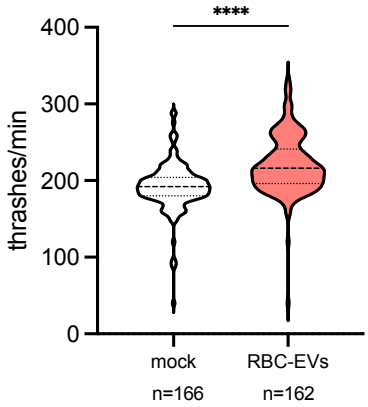

Figure 6. *Quantification of the number of thrashes after treatment with mock and RBC-EVs (20 ng/µL corresponding to 2e^7 particles/mL). Violin plots show the distribution of thrashes performed by the animals in a minute. Bold dashed lines in the centre correspond to the medians, while upper and lower dashed lines correspond to the quartiles. n is the number of animals analysed. t-test ****p<0.0001.*

5.2 RBC-EVs BIODISTRIBUTION AND STABILITY

RBC-EVs labelled with two different lipophilic dyes (Di-8-anepps and MemGlow) have been used to assess their uptake and biodistribution *in vivo*. Similarly to MSC-EVs, we observed that RBC-EV fluorescent signal was not visible after 24h of treatments and an exposure of at least 48h was needed to observe their internalization in worms. This strongly suggests that, unlike nanoalgosomes, mammalian derived EVs need more time to be up taken by *C. elegans* cells. After 48h of treatment a fluorescent signal was visible in the intestinal cells (Figure 7a) of all the animals, in the pseudocoelomic cavity and in coelomocytes (Figure 7b), suggesting that RBC-EVs have a tropism for the pseudocoelomic cavity. This is a cavity full of liquid that surrounds all the organs of the animal and contains 6 coelomocytes that are scavenger cells. Thus, the pseudocoelome can be somehow considered as a very primitive blood circuit. Interestingly and differently from nanoalgosomes, no fluorescent signal was observed in the head neurons, suggesting that different types of EVs can have different tissue tropism related to their intrinsic natural

This project has received funding from the European Union's Horizon 2020 research and innovation programme under grant agreement No 952183

composition. Nevertheless, RBC-EVs seem to be stable *in vivo* since the fluorescent signal was visible up to 24h after treatment interruption (Figure 7c).

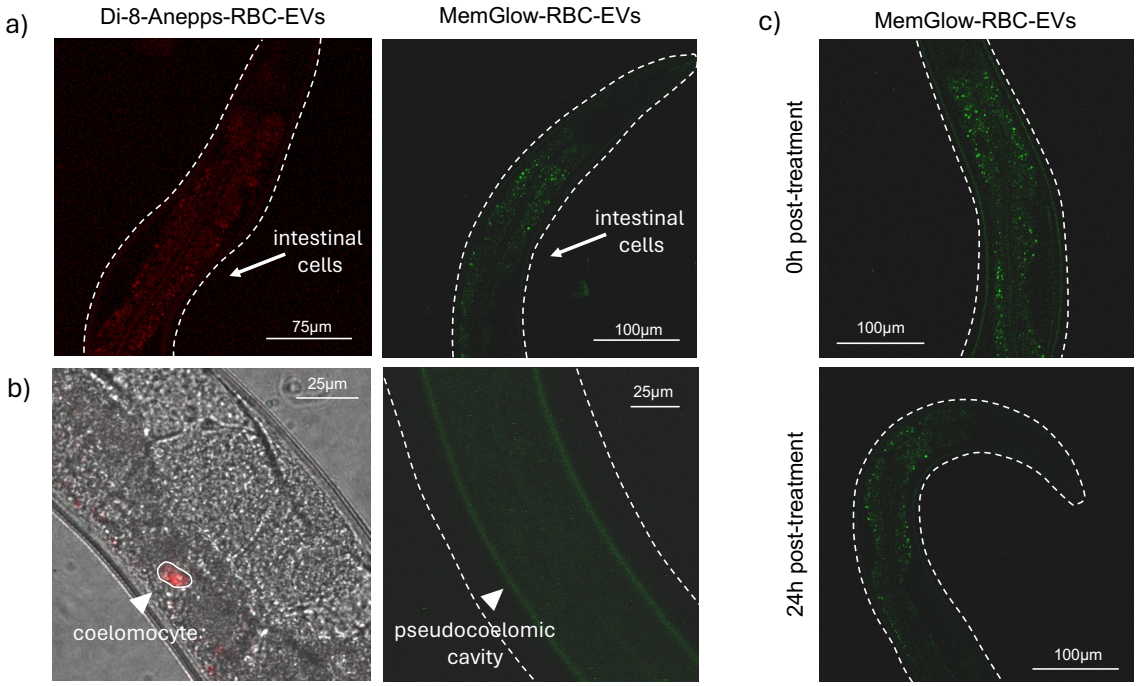

Figure 7. *a) Representative confocal images of animals treated with Di-8-anneps-RBC-EVs (red, left panel) and MemGlow-RBC-EVs (green, right panel). b) Representative confocal images of RBC-EVs localization in a coelomocyte (red, left panel) and pseudocoelomic cavity (green, right panel). c) Representative confocal images of animals treated with MemGlow-RBC-EVs (green) acquired after 0- and 24-hours post-treatment. RBC-EV concentration used was 20 ng/µL corresponding to 2e^{7} particles/mL. Animal body is outlined with white dashed lines, head is up. Scale bars are reported in the images.*

Taken together these results also support the use of RBC-EVs to encapsulate MBDs, especially considering the different tropisms and for personalised medicine, but further experiments on the biocompatibility are needed.

6. MBD PERFORMANCES *IN VIVO* IN *C. ELEGANS*

Single core magnetic bead devices (s.c. MBDs), specifically polydopamine-derivatized silica-coated superparamagnetic iron oxide nanoparticles provided by USC partner (WP2, D2.2, D2.5, and D2.6; Fe3O4@SiO2-PDA, hereafter referred as MBD-PDA) were evaluated for their biocompatibility and capability to induce oxidative stress. The results of these studies have been published together with the results obtained by other project partners (Romano *et al.*, 2023) and summarized in the present report. *C. elegans* animals have been exposed by soaking to a range of MBD-PDA concentrations (from 0.01 to 200 µg/mL) chronically from eggs to adult stage (72h). The tested mass of MBD-PDA corresponds to a range of 8.3x10^{9} – 2x10^{12} MBD-PDA per mL which could cover different EVs/MBD-PDA ratios for the final BOW hybrid products. Unfortunately, the functionalization with PDA did

This project has received funding from the European Union's Horizon 2020 research and innovation programme under grant agreement No 952183

not allow the visualization of MBD-PDA inside the animal, due to the endogenous autofluorescence of intestinal cells (Clokey *et al.*, 1986) emitting in the same wavelength of PDA (see below Figure 11).

6.1 MBD-PDA BIOCOMPATIBILITY

To assess MBD-PDA toxicity, animals were chronically exposed (72h) with very high MBD-PDA concentrations (100 and 200 µg/mL) and no effect on animal survival was observed (Figure 8a). To further characterize MBD-PDA biocompatibility, the animal fertility and embryonic survival were evaluated exposing animals with 50 µg/mL to avoid any aggregation of the MBD-PDA and also in this case no toxic effect was observed (Figure 8b and c). This result again confirms the absence of any transgenerational effect. However, a slight reduction in animal motility was observed using different concentrations (0.1, 1, 10 and 50 µg/mL) of MBD-PDA (Figure 8d), suggesting that MBD-PDA are more compatible than other iron-NPs in respect to the fitness of the animal, but they still cause a slight defect in locomotion.

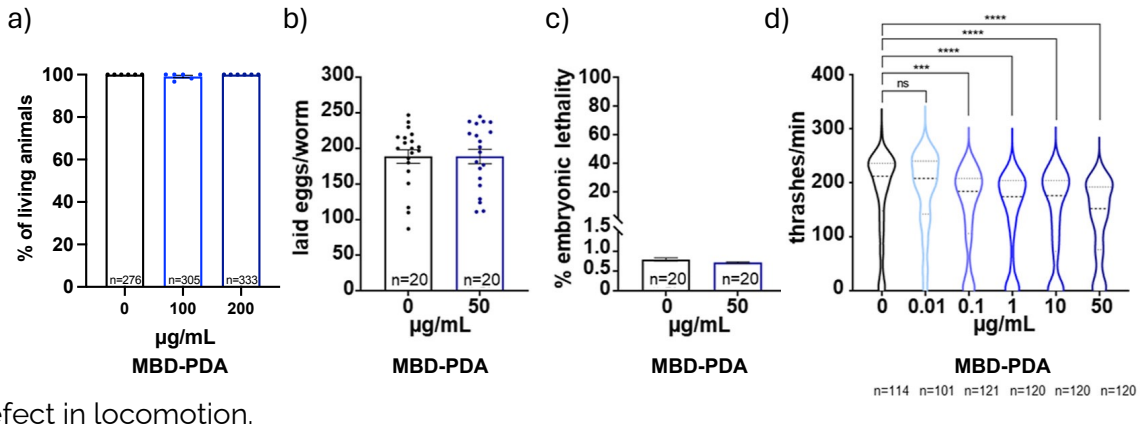

Figure 8. *a) Quantification of the number of living animals after treatment with mock (H_2O) or different MBD-PDA concentrations. b) Brood size of animals after treatment with mock and MBD-PDA. c) Embryonic lethality of animals after treatment with mock and MBD-PDA. d) Quantification of the number of thrashes after treatment with mock and different MBD-PDA concentrations. Bars represent the means and dots the replicates (a-c); error bar is the SEM. Violin plots (d) show the distribution of thrashes performed by the animals in a minute; bold dashed lines in the centre correspond to the medians, while upper and lower dashed lines correspond to the quartiles. n is the number of animals analysed (a and d) or the number of P0 animals (b), or the number of eggs analysed (c). MBD-PDA concentrations are reported in the graphs. t-test (b and c) and One-way ANOVA (a and d) have been used and only statistically significant differences have been reported ***p<0.005; ****p<0.0001, ns>0.05.*

6.2 MBD-PDA OXIDATIVE STRESS

Oxidative stress represents one of the biggest concerns in the use of MBDs. So MBD-PDA capability to induce an oxidative stress response *in vivo* was evaluated by using transgenic animals expressing the GFP under the promoter of *gst-4* gene, the ortholog of glutathione S-transferase (see above). Chronic exposure with MBD-PDA (50 µg/mL) indeed induces an oxidative stress response *in vivo* (Figure 9a and b). Taken together these results confirm

This project has received funding from the European Union's Horizon 2020 research and innovation programme under grant agreement No 952183

that MBD-PDA are more compatible than other iron-NPs for the fitness of the animal, but they still cause some toxicity and oxidative stress, that might be avoided by covering them with biological membranes.

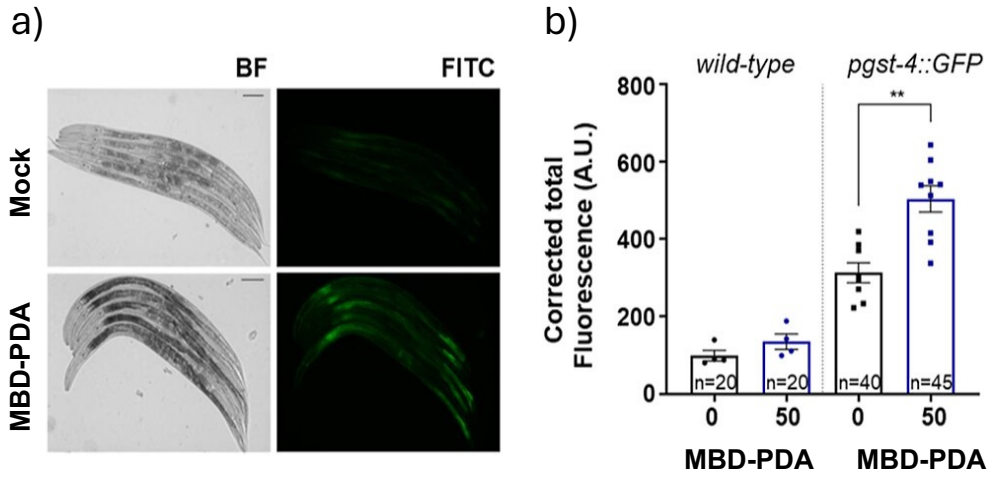

Figure 9. *a) Representative epifluorescence images of pgst-4::GFP expressing animals after chronic treatment with mock (H_2O) or MBD-PDA. Scale bar is 75 µm. Heads are on the left. b) Quantification of the fluorescence in pgst-4::GFP expressing animals after chronic treatment with mock or MBD-PDA. Bars represent the means and dots the total fluorescence in a picture corrected for the background; error bar is the SEM. MBD-PDA concentration used 50 µg/mL. t-test **p<0.001.*

7. LIPOSOME-MEMBRANE COATED MBDs VERSUS MBDs *IN VIVO* IN *C. ELEGANS*

Silica embedded single core and multicore superparamagnetic iron oxide nanoparticles functionalized with rhodamine B isothiocyanate (RITC) (MBD-RITC), provided by USC partner (D2.5; MGAP19 single core and AP20 multicore; Acevedo *et al.*, 2022) were coated with liposome-membrane (lpMBD) by CSGI partner. As reported in D5.4, lpMBDs were introduced (see T3.e) to support Task 3.3 in producing the evMBDs and to validate T3.1 and T3.2 approaches. Nanoparticles were functionalized with rhodamine B isothiocyanate in order to visualize them *in vivo* (see below). For the generation of the lpMBD prototypes MGAP19 were selected as single-core MBDs (sc MBDs), while AP20 were used as multi-core MBDs (mc MBDs) (D2.5, D2.6).

7.1 lpMBD VS MBD BIOCOMPATIBILITY

Based on the experiments described in section 5.1, the MBD and lpMBD effect was evaluated on animal movement. Empty liposomes were demonstrated to have no effect on animal thrashing and the results of these studies have been published together with other project partners (Paterna *et al.*, 2023). Consistently with previous tests on MBD-PDA, also MBD-RITC decreased animal movement after a chronic treatment at 50 µg/mL, whether we used single or multi core nanoparticles (Figure 10). Interestingly, lpMBDs did not alter animal movement, suggesting that liposome coating protects animals from MBD toxicity.

This project has received funding from the European Union's Horizon 2020 research and innovation programme under grant agreement No 952183

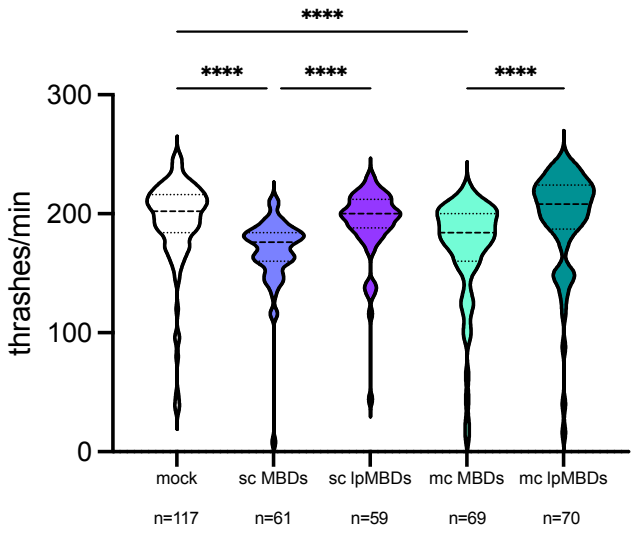

Figure 10. *Quantification of the number of thrashes after treatment with mock (H_2O), sc MBD, sc lpMBD, mc MBD and mc lpMBD. Violin plots show the distribution of thrashes performed by the animals in a minute. Bold dashed lines in the centre correspond to the medians, while upper and lower dashed lines correspond to the quartiles; n is the number of animals analysed. MBD concentration used is 50 µg/mL. One-way ANOVA **** p<0.0001.*

7.2 lpMBD VS MBD BIODISTRIBUTION

As stated before, the functionalization with PDA did not allow the visualization of MBDs inside the animals, due to the endogenous autofluorescence of *C. elegans* intestinal cells (Clokey *et al.*, 1986) that emit in the same wavelength of PDA (arrowhead Figure 11a).

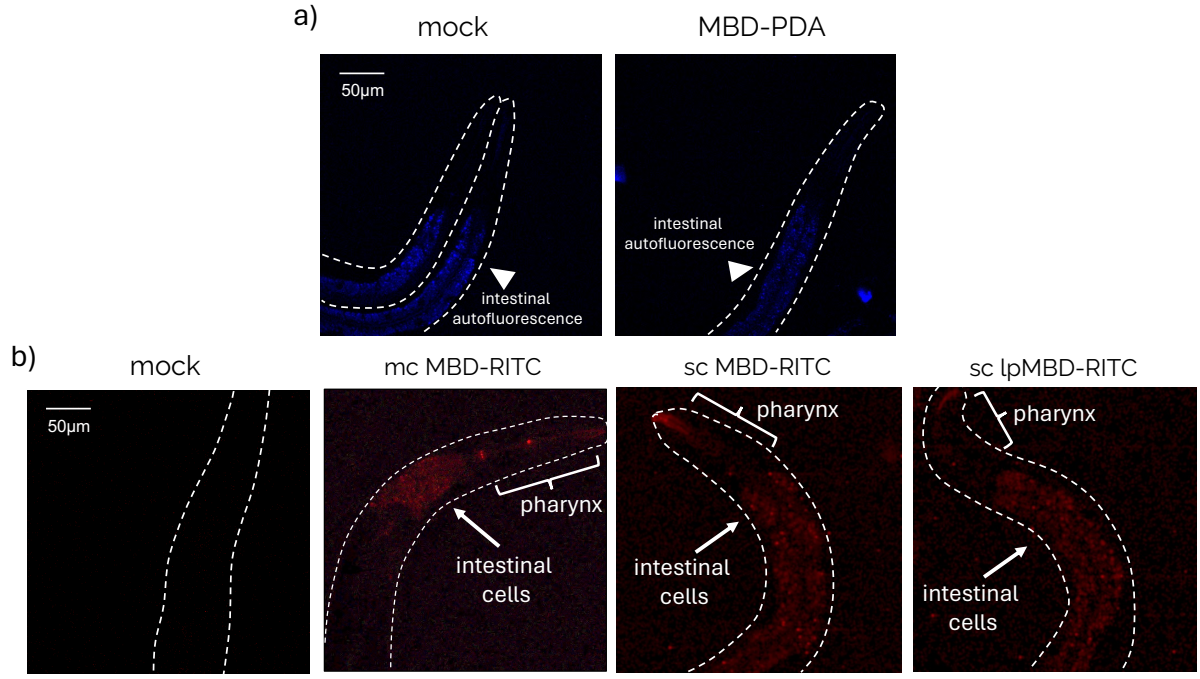

Figure 11. *a) Representative confocal images of animals treated with mock (H_2O) or MBD-PDA. b) Representative confocal images of animals treated with mock, mc MBD-RITC, sc MBD-RITC and sc lpMBD-RITC. MBD concentrations used are 50 µg/mL. Animal body is outlined with white dashed lines, heads are up. Scale bars are reported in the images.*

This project has received funding from the European Union's Horizon 2020 research and innovation programme under grant agreement No 952183

To overcome this issue, MBDs have been functionalized with RITC, having a fluorescence spectrum non overlapping with the autofluorescence of *C. elegans* intestinal cells, as observed in Figure 11b. After 24h exposure with MBDs and lpMBDs a specific fluorescent signal was observed in the pharynx (bracket) and in the intestinal cells (arrow) of all the animals (Figure 11b). Interestingly, liposomes coating did not alter MBDs localization inside the animal.

7.3 lpMBD VS MBD PERSISTENCE

MBDs and lpMBDs persistence was then assessed by looking at the fluorescent signal 24 h post treatment and also in this case similar internalization signals were observed. Further experiments have been performed to understand the different effect of MBDs and lpMBDs on animal movement (section 6.1), assessing their effects 24- and 48-hours after the end of treatment, thus supposing a delayed effect. After 24h post-treatment MBDs reduced animal movement, while lpMBDs did not, similarly to what observed after 0h post-treatment. Interestingly, at 48 h post-treatment a similar decrease in animal movement was observed with either MBDs or lpMBDs (162 vs 154 thrashes/minute, n>65, not statistically significant difference), suggesting that covering MBDs with liposomes delays the toxic effect of MBDs. To exclude that the difference observed were related to a different iron internalization, we quantified total iron in treated animals by inductively couple plasma atomic emission spectroscopy (ICP-AES). Animals were analyzed after 0h and 48h post-treatment and total iron content per animal was quantified. Preliminary results suggest that no differences in the amount of internalized iron are visible, confirming that the effects observed are not related to differences in iron internalization.

Taken together these results confirm that lpMBDs are more compatible than uncovered ones for the fitness of the animal, showing a delay in toxicity. This effect might be improved by encapsulating MBDs in EV derived membranes.

8. CONCLUSIONS

This deliverable describes the results obtained *in vivo* in the model system *C. elegans* regarding the biocompatibility and biodistribution of BOW products building-block materials, and of a prototype hybrid. The overall results suggested a good biocompatibility of all types of EVs analyzed and a mild toxicity of MBDs *in vivo* in *C. elegans.* Interestingly, all the BOW products showed a specific intestinal localization, and interestingly different types of EVs can have a different tropism. Importantly, among all BOW products, MBDs are the only ones that have some, albeit moderate, toxicity in vivo in *C. elegans*. This strongly supports their use as a benchmark to test membrane cating as a tool to decrease/delay the toxicity. Indeed, experiments with lpMBDs did show a delay of MBDs toxic effect, supporting the idea that membrane coating can improve biocompatibility of synthetic nanodevices and encourage for their possible safe use in pharmaceutical applications. The experiments described in this deliverable allowed a deep and rapid evaluation of BOW products performances *in vivo,* in an invertebrate model system, dissecting the molecular mechanisms through genetics, as well as

This project has received funding from the European Union's Horizon 2020 research and innovation programme under grant agreement No 952183

showing the uptake and biodistribution in a living animal, with no sacrifice of higher animals. Thus, the broad spectrum of experiments performed in *C. elegans* as first *in vivo* screening allowed and will allow the consortium to extrapolate useful information to refine their experimental plan, also in order to reduce the use of mammalian animal models.

9. REFERENCES

- Acevedo PG, González Gómez MA, Arnosa Prieto A, De Castro Alves L, Seco Gudiña R, Piñeiro Y, Rivas J. Fluorescent Single-Core and Multi-Core Nanoprobes as Cell Trackers and Magnetic Nanoheaters. Magnetochemistry. 2022. 8(8), 83. doi: 10.3390/magnetochemistry8080083
- Bongiovanni A., Adamo G, Santonicola P, et al. Microalgae as a novel biofactory for biocompatible and bioactive extracellular vesicles, 17 October 2023, PREPRINT (Version 1) available at Research Square [https://doi.org/10.21203/rs.3.rs-2841234/v1]
- Brenner S. The genetics of *Caenorhabditis elegans*. *Genetics* 1974, *77* (1), 71–94. https://doi.org/10.1093/genetics/77.1.71.
- Clokey GV and Jacobson LA. The autofluorescent "lipofuscin granules" in the intestinal cells of Caenorhabditis elegans are secondary lysosomes. Mech Ageing Dev. 1986 Jun;35(1):79-94. doi: 10.1016/0047-6374(86)90068-0.
- Musicò A, et al. Surface functionalization of extracellular vesicle nanoparticles with antibodies: a first study on the protein corona "variable." Nanoscale Adv. 5, 4703–4717 (2023).
- Paterna A, Santonicola P, Di Prima G, Rao E, Raccosta S, Zampi G, Russo C, Moran O, Manno M, Di Schiavi E, Librizzi F, Carrotta R. αS1-Casein-Loaded Proteo-liposomes as Potential Inhibitors in Amyloid Fibrillogenesis: In Vivo Effects on a C. elegans Model of Alzheimer's Disease. ACS Chem Neurosci. 2023 Nov 1;14(21):3894-3904. doi: 10.1021/acschemneuro.3c00239.
- Picciotto S, Santonicola P, Paterna A, Rao E, Raccosta S, Romancino DP, Noto R, Touzet N, Manno M, Di Schiavi E, Bongiovanni A, Adamo G. Extracellular vesicles from microalgae: uptake studies in human cells and Caenorhabditis elegans. Front Bioeng Biotechnol. 2022 Mar 24:10:830189. doi: 10.3389/fbioe.2022.830189. eCollection 2022. doi: 10.3389/fbioe.2022.830189
- Plaza M, Herrero M, Cifuentes A, Ibáñez E. Innovative Natural Functional Ingredients from Microalgae. J Agric Food Chem 2009, 57 (16), 7159–7170. doi:10.1021/jf901070g.
- Romano M, González Gómez MA, Santonicola P, Aloi N, Offer S, Pantzke J, Raccosta S, Longo V, Surpi A, Alacqua S, Zampi G, Dediu VA, Michalke B, Zimmerman R, Manno M, Piñeiro Y, Colombo P, Di Schiavi E, Rivas J, Bergese P, Di Bucchianico S. Synthesis and Characterization of a Biocompatible Nanoplatform Based on Silica-Embedded SPIONs Functionalized with Polydopamine. ACS Biomater Sci Eng. 2023 Jan 9;9(1):303-317. doi: 10.1021/acsbiomaterials.2c00946.
- Sugawara T, Sakamoto K. Quercetin Enhances Motility in Aged and Heat-Stressed Caenorhabditis Elegans Nematodes by Modulating Both HSF-1 Activity, and Insulin-like and P38-MAPK Signalling. PLoS One 2020, 15 (9), e0238528. doi:10.1371/journal.pone.0238528

This project has received funding from the European Union's Horizon 2020 research and innovation programme under grant agreement No 952183